ON THE RESOLUTION LIMITS OF SUPERIMPOSED PROJECTION

Niranjan Damera-Venkata and Nelson L. Chang

Imaging Technology Department, Hewlett-Packard Labs, Palo Alto CA 94304 USA
{niranjan.damera-venkata | nelson.chang} @ hp.com

ABSTRACT

Multi-projector super-resolution is the dual of multi-camera super-resolution. The goal of projector super-resolution is to produce a high resolution frame via superimposition of multiple low resolution subframes. Prior work claims that it is impossible to improve resolution via superimposed projection except in specialized circumstances. Rigorous analysis has been previously restricted to the special case of uniform display sampling, which reduces the problem to a simple shift-invariant deblurring. To understand the true behavior of superimposed projection as an inverse of classical camera super-resolution, one must consider the effects of non-uniform displacements between component subframes. In this paper, we resolve two fundamental theoretical questions concerning resolution enhancement via superimposed projection. First, we show that it is possible to reproduce frequencies that are well beyond the Nyquist limit of any of the component subframes. Second, we show that non-uniform sampling and pixel reconstruction functions impose fundamental limits on achievable resolution.

Index Terms— super-resolution, superimposed projection, image display, alias cancellation, non-uniform sampling

1. INTRODUCTION

Classic camera super-resolution seeks to reconstruct a high resolution image given several camera captured low resolution images [1]. Superimposed projection is the dual problem of generating multiple low resolution images (called subframes) given a desired high resolution image. The low resolution images are superimposed to approximate the desired high resolution image. Examples of superimposed projection include Wobulation [2] and multi-projector superimposition [3, 4, 5]. In Wobulation, multiple low resolution subframes of data are generated from each high resolution frame of image data. An optical image shifting mechanism jitters the projected image of each subframe by a sub-pixel shift. The subframes are projected in rapid succession so as to appear as if they were projected simultaneously and superimposed. In multi-projector superimposition, the output of multiple low resolution projectors are aligned using camera-based registration. The geometric displacement between subframes may be modeled with shifts [3] or with more general geometric transformations [5, 4].

In general, the grid of pixel centers formed by the superimposition of two or more uniform (or possibly geometrically distorted) grids is non-uniform (see Fig. 1). Previous work has shown the viability of super-resolution only in the special case when the grid is uniform. Majumder [6] claimed to show that resolution enhancement is impossible except when the superimposed grid was uniform and when pixel sizes are such that no overlap between pixels is allowed. Said [7] rigorously analyzed 1-D superimposed projection

(a) subframes (b) superimposed result

Fig. 1. Superimposed projection.

when the grid of superimposed pixel centers is uniform and critically sampled (i.e. the high resolution image to be reproduced has the same number of pixels as the superimposed grid). In this case, the problem of determining the optimal subframes reduces to shift invariant pre-filtering on the uniform grid, to undo the effect of the pixel point spread function. By analyzing the properties of the resulting deblurring filters, Said showed that the optimal inverse filters result in increasing amplification of high-frequencies which produces signals that are beyond the projectors' range of possible inputs. This showed that although resolution gain is possible, there are limits to the maximum achievable resolution even in this special case. However, the dual of this problem is image deblurring (which is a post-filtering operation) and not classic super-resolution.

In contrast, this paper addresses the real dual to classic super-resolution, by examining the mechanism of resolution enhancement via superimposed projection with non-uniform sampling geometries. A 1-D superimposition filter bank model is presented in Section 3.1 to properly analyze the more general non-uniform case. We establish the fundamental theory governing resolution enhancement and alias cancellation in the non-uniform sampling case (Sections 3 and 4). We present practical limits to achievable resolution (Section 5) as well as experimental results with 2-D images (Section 6).

The importance of developing theory addressing the more general non-uniform case should be stressed. For Wobulation systems, cheaper image shifting mechanisms may be designed if the restriction on precise uniform grids is removed. For multi-projector superimposition, the superimposed grid is almost always non-uniform. Finally, there are limited uniform grid configurations with N subframes in the 2-D case, and improved image quality may be achieved in practice by non-uniform oversampling [8].

2. MODELING 1-D SUPERIMPOSITION

Fig. 2 shows our 1-D model of superimposed projection consisting of N component image projectors. The k^{th} component image projector is driven with low resolution subframe $y_k[n]$, upsampled by a factor M, filtered using discrete filter $\tilde{R}(\omega)$, and then offset with respect to the zeroth image projector by a global shift t_k. The shift is represented in the frequency domain by a multiplication with the factor $e^{-j\omega t_k}$. The shifted signals from the component image pro-

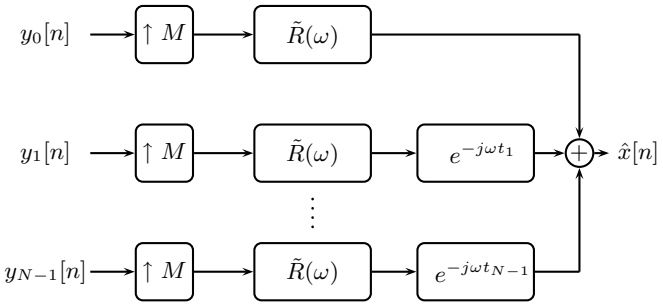

Fig. 2. Discrete model for 1-D superimposed projection.

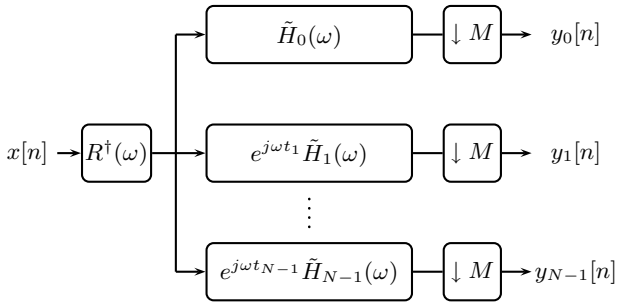

Fig. 3. Analysis filter bank for optimal subframe generation.

jectors are summed to obtain a discrete simulation $\hat{x}[n]$ of the superimposed signal. We assume that there is no variation in pixel profiles or brightness among the component image projectors.

The above model accounts for display sampling, non-uniform geometric distortion between component image projectors, and pixel profiles. These quantities are the key determinants of image quality. In the case of finite extent signals, the entire model may be expressed using discrete linear operators as:

$$\hat{\mathbf{x}} = \sum_{k=0}^{N-1} \mathbf{S}_{t_k}\, \mathbf{R}\, \mathbf{D}_M^T\, \mathbf{y}_k = \mathbf{R} \underbrace{\sum_{k=0}^{N-1} \mathbf{S}_{t_k}\, \mathbf{D}_M^T\, \mathbf{y}_k}_{\hat{\mathbf{z}}} \qquad (1)$$

The up-sampling operation is modeled by the matrix operator $\mathbf{D}_M^T$, the transpose of the downsampling operator $\mathbf{D}_M$. Reconstruction is modeled by the Toeplitz matrix $\mathbf{R}$. Relative fractional shift between the component projectors is represented by the linear operator matrix $\mathbf{S}_{t_k}$ that models a fractional delay.

In the case of uniform critical sampling, $\hat{\mathbf{x}}$ may be formed by first rearranging sample values on the high resolution grid and then filtering with the reconstruction filter. In this case, $\hat{\mathbf{z}}$ represents a uniform grid of all subframe sample values $\mathbf{y}_k$, $\forall k$ with no missing grid points. Thus, the optimal subframe values may be obtained by a simple deblurring of the reconstruction filter. There is no aliasing introduced in the uniform critically sampled case and hence, no need for explicit alias elimination.

In contrast, for the more general case of non-uniform sampling, the grid on which $\hat{\mathbf{z}}$ is formed has gaps. This means that the mapping between the collection of subframe pixels on the high resolution grid and $\hat{\mathbf{x}}$ is not LTI. Hence, one cannot recover the optimal subframe values by simple inverse filtering. If the subframes $\mathbf{y_k}$ are not properly generated, the term $\hat{\mathbf{z}}$ will contain aliasing that cannot be undone even if the reconstruction filter could be perfectly inverted.

We propose viewing the optimal subframe generation process as an analysis filter bank that attempts to both undo the effects of $\tilde{R}(\omega)$ and cancel the aliasing due to the non-uniform shifts $e^{-j\omega t_k}$; Fig. 3 shows the analysis bank with regularized pseudo-inverse filter $\tilde{R}^{\dagger}(\omega)$ to counter $\tilde{R}(\omega)$ and analysis filters $\tilde{H}(\omega)$ to cancel aliasing. This filter bank framework thus facilitates a proper analysis of the non-uniform sampling case and alias cancellation. When $N = M$, the filter bank is a non-uniform maximally decimated bank, for which we can derive the optimal alias cancellation filters in closed form (Section 3). When $N > M$, the filter bank is a non-uniform oversampled filter bank with more pixels in the superimposed image than present in the original high resolution image. In this case, we can derive the optimal alias cancellation filters as the limit of an operator sequence (Section 4).

3. ALIAS CANCELLATION IN MAXIMALLY DECIMATED SUPERIMPOSED PROJECTION

When the filter bank is maximally decimated (i.e. $N = M$), the optimal analysis filter coefficients may be derived in closed form as shown by the following theorem.

Theorem 3.1 *A high resolution signal $x[n]$ can be split into N low resolution subframes $y_k[n]$, $k = 0, 1, ...N-1$ by filtering with an analysis bank of filters $\tilde{h}_k[n]$ followed by decimation by N. The signals $y_k[n]$ can be designed to exactly reproduce $x[n]$, when up-sampled by N and superimposed with distinct relative shift offsets $t_k < N$. The optimal subframes $y_k[n]$ may be generated using the following equations:*

$$w_k[n] = sinc(n + t_k) \qquad (2)$$

$$a_k = \frac{1}{\prod_{q=0, q\neq k}^{N-1} \sin\left(\pi\left(t_q - t_k\right)/N\right)} \qquad (3)$$

$$f_k[n] = a_k \frac{\prod_{q=0}^{N-1} \sin\left(\pi\left(n + t_q - t_k\right)/N\right)}{\pi n/N} \qquad (4)$$

$$\tilde{h}_k[n] = \sum_p f_k[p]\; w_k[n-p] \qquad (5)$$

$$y_k[n] = \sum_p \tilde{h}_k[p]\; x[nN-p] \qquad (6)$$

The filter $w_k[n]$ is the impulse response of an ideal fractional delay filter [9]. The proof of the above theorem is omitted due to space restrictions. However, we validate the result by simulation.

Example 3.1 *Let $N = 2$, $t_0 = 0$ and $t_1 = 0.5$. Let $x[n] = A((\cos(2\pi f n) + 1)/2) + (0.5 - A/2)$ with $A = 0.5$ and normalized frequency $f = 0.4$. The input signal frequency is beyond the Nyquist frequency of any of the subframes (viz. 0.25).*

This configuration is the same one analyzed in [6], where it was incorrectly concluded that aliasing could not be eliminated. To the contrary, we demonstrate that aliasing effects of the non-uniform sampling may indeed be cancelled by a proper choice of subframes to produce alias-free super-Nyquist frequencies. Fig. 4(a) shows the two aliased subframes $y_k(t)$, and Fig. 4(b) shows the reconstructed $\hat{x}(t)$.[1] Despite $y_k(t)$ being aliased, $x(t)$ and $\hat{x}(t)$ are found to be

[1] All discrete signals have been reconstructed with ideal sinc interpolation at an $8\times$ oversample factor relative to $x[n]$. This step eliminates post-aliasing

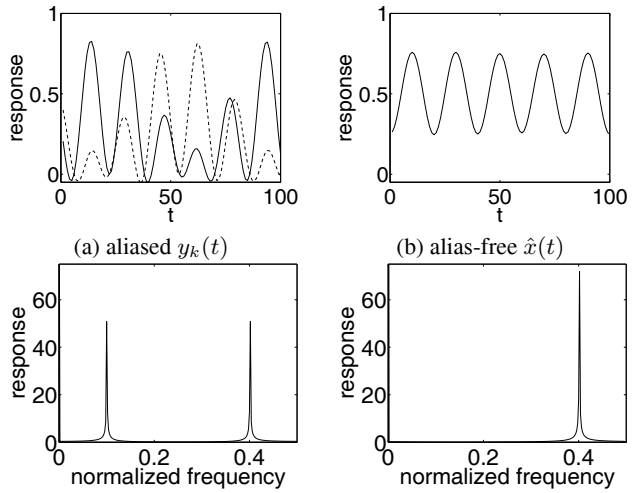

(a) aliased $y_k(t)$ (b) alias-free $\hat{x}(t)$

(c) $Y_k(\omega)$ (d) $\hat{X}(\omega)$

Fig. 4. Super-Nyquist results of Example 3.1.

virtually identical. The alias cancellation can also be clearly seen in the frequency domain where the subframes in Fig. 4(c) have an alias component at $f = 0.1$ that is eliminated in the superimposed result of Fig. 4(d).

4. ALIAS CANCELLATION IN OVERSAMPLED SUPERIMPOSED PROJECTION

When the filter bank is oversampled (i.e. $N > M$), there is no unique choice of closed-form alias cancellation filters. Nevertheless, the optimal estimates for the subframes $\{\mathbf{y}_k^*\}$ may be obtained as solutions to the following optimization problem:

$$\{\mathbf{y}_k^*\} = \underset{\{\mathbf{y}_k\}}{\operatorname{argmin}} \|\mathbf{x} - \sum_k \mathbf{S}_{t_k}\, \mathbf{D}_M^T\, \mathbf{y}_k\|^2 \tag{7}$$

Note the reconstruction operator $\mathbf{R}$ is not included above since we are interested in analyzing the effects of alias cancellation alone. The optimization problem of Eq. (7) may be solved using the following iterative algorithm.

$$\mathbf{y}_k^{(0)} = \mathbf{D}_M\, \mathbf{S}_{t_k}^T\, \mathbf{x} \tag{8}$$

$$\hat{\mathbf{x}}^{(n)} = \sum_{k=0}^{N-1} \mathbf{S}_{t_k}\, \mathbf{D}_M^T\, \mathbf{y}_k^{(n)} \tag{9}$$

$$\frac{\partial J}{\partial \mathbf{y}_k^{(n)}} = -\mathbf{D}_M\, \mathbf{S}_{t_k}^T \left(\mathbf{x} - \hat{\mathbf{x}}^{(n)}\right) \tag{10}$$

$$\mathbf{y}_k^{(n+1)} = \mathbf{y}_k^{(n)} - \mu\, \frac{\partial J}{\partial \mathbf{y}_k^{(n)}} \tag{11}$$

$$\{\mathbf{y}_k^*\} = \lim_{n\to\infty} \{\mathbf{y}_k^{(n)}\} \tag{12}$$

where μ is the step-size of the descent algorithm. The iterative process is guaranteed to converge to an optimal choice of subframes due to convexity and can be shown to be equivalent to an analysis bank of filters followed by downsampling [4, 5]. The iterative filter bank subframe generation also optimally cancels aliasing.

artifacts introduced by MATLAB's default connect-the-dots reconstruction. Also, the infinite impulse responses of Theorem 3.1 were truncated using appropriate Hamming windows for the implementation.

5. ANALYSIS OF RESOLUTION LIMITS

In the section, we consider practical range limits on the subframes by way of a couple of examples. While Section 3 presented an optimal closed-form solution to cancel aliasing for $N = M$, it does not guarantee that the subframes will all be in the range [0,1] (Example 3.1 happened to have $y_k[n] \in [0, 1]$).

To overcome this issue, one can impose limit constraints in the iterative algorithm of Section 4 by clipping the updates of Eq. (11) to the range $[0, 1]$ at each iteration. Since this is a projection onto a convex constraint set, the algorithm still converges to an optimal solution, and has the added benefit of ensuring practical limits on subframes $y_k[n]$.

Example 5.1 *Consider the signal of Example 3.1 with $A = 0.6$, $N = 2$, $t_0 = 0$, $t_1 = 0.1$, $f = 0.4$*

We examine using the closed form solution of Section 3 for this case. Although the reconstructed signal (Fig. 5(b)) is alias-free, subframe $y_1[n]$ clearly exceeds its operating range [0,1] (Fig. 5(a)). If we instead use the iterative algorithm and optimize the subframes subject to practical limit constraints (Fig. 5(c)), the reconstructed signal is unable to cancel the aliasing entirely (Fig. 5(d)) with just $N = 2$ subframes.

Example 5.2 *Consider the signal of Example 3.1 with $A = 0.6$, $N = 4$, $t_0 = 0$, $t_1 = 0.1$, $t_2 = 0.5$, $t_3 = 0.7$ and $f = 0.4$*

We consider simply introducing two additional component projectors so that $N = 4 > M$. In this case, the computed subframe $y_1[n]$ does not exceed the range [0,1] (Fig. 6(a)), and the reconstructed signal after applying the iterative algorithm sufficiently cancels the aliasing (Fig. 6(b)). Thus through oversampling, we demonstrate the ability to overcome aliasing in the reconstructed signal while ensuring individual subframes lie in their operating range. Note that in practice, oversampling also helps by reducing post-aliasing reconstruction artifacts due to non-ideal pixel PSFs even at sub-Nyquist frequencies [4, 5].

Up to this point, we have considered only the effects of the non-uniform sampling and alias cancellation. The reconstruction filter imposes independent limits since we cannot undo the blur exactly in most cases [7]. In general, increased oversampling allows for better alias cancellation and the resolution is limited by our ability to deblur the reconstruction filter. Clearly, if the low resolution pixel bandwidth is not greater than the Nyquist frequency of a low resolution subframe, no super-resolution is possible. If however, the low resolution pixel has a bandwidth greater than the Nyquist frequency of the low resolution subframe (most practical pixel PSFs have this property), each low resolution image can be engineered to contribute frequencies higher than its Nyquist frequency without violating the laws of superimposition, meaning that each subframe will have low-frequency aliasing. We have demonstrated that by properly generating the complementary subframes, we can cancel the low-frequency aliasing and reconstruct alias-free high frequencies that are beyond the Nyquist frequency of a single projector subject to physical range limits. For a given configuration, the amplitudes of sinusoids at various frequencies that the system can reconstruct without aliasing is a measure of achievable resolution.

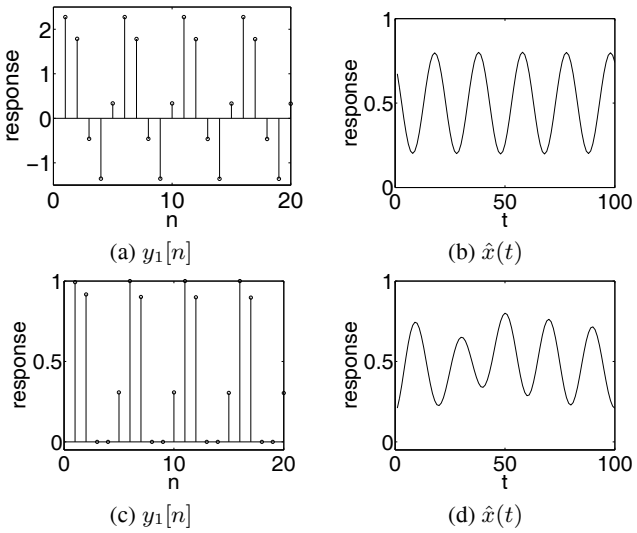

Fig. 5. Effect of subframe clipping in Example 5.1.

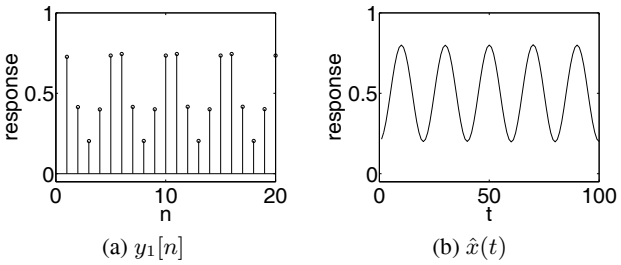

Fig. 6. Effect of oversampling in Example 5.2.

6. EXTENSIONS TO 2-D IMAGES

While the discussion has focused on 1-D models, it may be naturally extended to 2-D images and applied to real systems. Fig. 7 presents actual results from experimental multi-projector superimposition systems for $M = 2$. The results were generated using a practical extension of the iterative algorithm of Section 4 to simultaneously incorporate deblurring and alias cancellation [4]. The first example shows a representative aliased subframe (Fig. 7(a)) and its corresponding alias-free super-Nyquist result (Fig. 7(b)) for $N = 4$. Even more dramatic improvement may be observed in the second example (Figs. 7(c) and (d)) for $N = 10$.

7. CONCLUSIONS

We showed that superimposed projection can be modeled using non-uniform filter banks. In this more general case, the optimal signal generation problem reduces to the optimal choice of analysis filters to 1) cancel the aliasing introduced by the non-uniform sampling, and 2) deblur the pixel reconstruction function. We showed both theoretically and via simulation that signal frequencies well beyond the Nyquist frequency of an individual subframe may be accurately reproduced by using a well-designed subframe generation algorithm. However, there are limits due to the finite signal ranges of the subframes in practical cases. We demonstrated that the reconstruction filter and the sampling may independently cause the signal limits to be exceeded, making it practically impossible to perfectly reproduce all input signal frequencies and amplitudes. Nevertheless, significant gains are indeed achievable through superimposed projection.

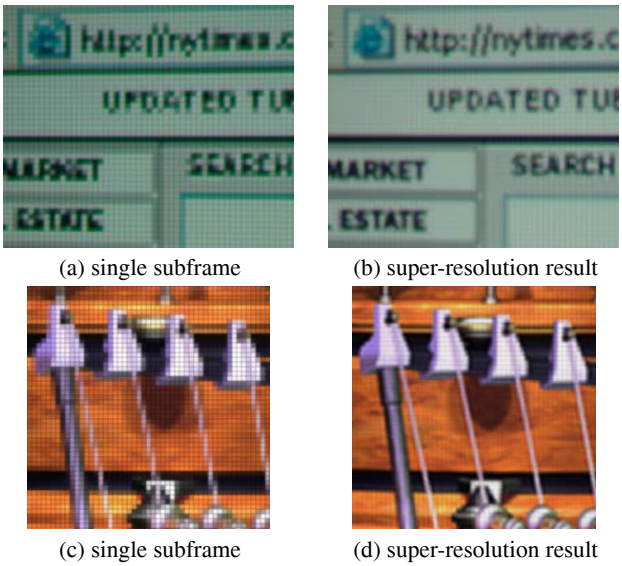

Fig. 7. Examples of resolution gain via superimposed projection.

8. REFERENCES

[1] S. Park, M. Park, and M. Kang, "Super-resolution image reconstruction: A technical overview," *IEEE Signal Processing Mag.*, vol. 20, pp. 21–36, May 2003.

[2] W. Allen and R. Ulichney, "Wobulation: Doubling the addressed resolution of projection displays," in *Proc. SID Symposium Digest of Technical Papers (SID)*, Boston, MA, May 2005, pp. 1514–1517.

[3] C. Jaynes and D. Ramakrishnan, "Super-resolution composition in multi-projector displays," in *Proc. IEEE International Workshop on Projector-Camera Systems (ProCams)*, Nice, France, Oct. 2003.

[4] N. Damera-Venkata and N. L. Chang, "Realizing super-resolution with superimposed projection," in *Proc. IEEE International Workshop on Projector-Camera Systems (ProCams)*, Minneapolis, MN, June 2007.

[5] N. Damera-Venkata and N. L. Chang, "Display supersampling," *ACM Transactions on Computer Graphics*, In submission.

[6] A. Majumder, "Is spatial super-resolution feasible using overlapping projectors?," in *Proc. IEEE International Conference on Acoustics, Speech, and Signal Processing (ICASSP)*, Philadelphia, USA, Mar. 2005, pp. 209–212.

[7] A. Said, "Analysis of subframe generation for superimposed images," in *Proc. IEEE International Conference on Image Processing (ICIP)*, Atlanta, GA, Oct. 2006, pp. 401–404.

[8] J. Foley, A. Van Dam, S. Feiner, and J. Hughes, *Computer Graphics: Principles and Practice*, Addison-Wesley, Reading, MA, 1990.

[9] T. Laakso et al., "Splitting the unit delay," *IEEE Signal Processing Mag.*, vol. 13, pp. 30–60, Jan. 1996.